Standard Article

International Journal of
ENGINE RESEARCH

Analysis of an innovative combustion chamber with the wall guided fuel injection in a small diesel engine

İlker Temizer[1] , **Öncel Öncüoğlu**[2] **and Ömer Cihan**[3]

Abstract

This paper has included the effects of different bowl geometries which has the wall guided fuel injection. Bowl geometries, which affect in-cylinder air flows, have a great influence on the change of mixture formation. Also, the region where the fuel hits in the bowl affects all engine parameters. In this presented numeric study, the standard combustion chamber geometry of a single-cylinder, air-cooled, and direct-injection diesel engine is compared with the designed new combustion chamber. Four different rotation angles (0°, 7.5°, 10°, and 15°) were determined for the new combustion chamber geometry and compared with the standard geometry. The three-dimensionally modeled bowl geometries in 3D Computational Fluid Dynamics simulation were examined in terms of in-cylinder pressure and temperature, instantaneous and cumulative heat release rate, exhaust emissions (NO, soot, CO, and CO_2), temperature/spray, and equivalence ratio/spray at different CA's. The effects of the different rotation angles of the designed new bowl geometry on both the air movement and the region where the fuel hits were investigated for the engine parameters. When the results obtained are examined, maximum in-cylinder pressures for standard combustion chamber, new combustion chamber 1, new combustion chamber 2, new combustion chamber 3, and new combustion chamber 4 geometries were obtained 79.5, 75.2, 78, 78.1, and 78 bar respectively, and the maximum in-cylinder temperatures were found 1766, 1742, 1805, 1817, and 1818 K, respectively. According to the results obtained from the numerical analysis, CO, CO_2, and soot emissions decreased while NO emissions increased in the new combustion chamber, compared to the standard combustion chamber. Examined the spray distributions in bowl, it was seen that the fuel sprays distributed more homogeneously and flame propagates which is spread throughout the chamber in the new combustion chamber type, which improved the mixture formation. The wall guided fuel flow in the novel designed chamber geometries beneficial to turbulence kinetic energy, spray distribution, emissions.

Highlights

- New combustion chamber is designed in this study.
- It was improved the mixture formation in the combustion chamber. In addition, a more homogeneous mixture was obtained by providing the distribution of the fuel assembly to more than one region.
- While lower soot, CO and CO_2 were obtained with NCC bowl geometries than the SCC type, NO emissions increased.
- In the new design types, it is observed that there is a slight decrease in the combustion pressure. This situation causes to run more silently and smoothly of the engine, resulting in a decrease in thermal and mechanical loads on the engine parts.

Introduction

Restrictions in emission regulations and high performance expectations of drivers have revealed the necessity of investigating the combustion phenomenon in

[1]Department of Manufacturing Engineering, Sivas Cumhuriyet University, Sivas, Turkey
[2]Department of Mechanical Engineering, Istanbul Technical University, İstanbul, Turkey
[3]Department of Machinery and Metal Technologies, Hendek Vocational School, Sakarya University of Applied Sciences, Sakarya, Turkey

Corresponding author:
İlker Temizer, Department of Manufacturing Engineering, Sivas Cumhuriyet University, Sivas 58140, Turkey.
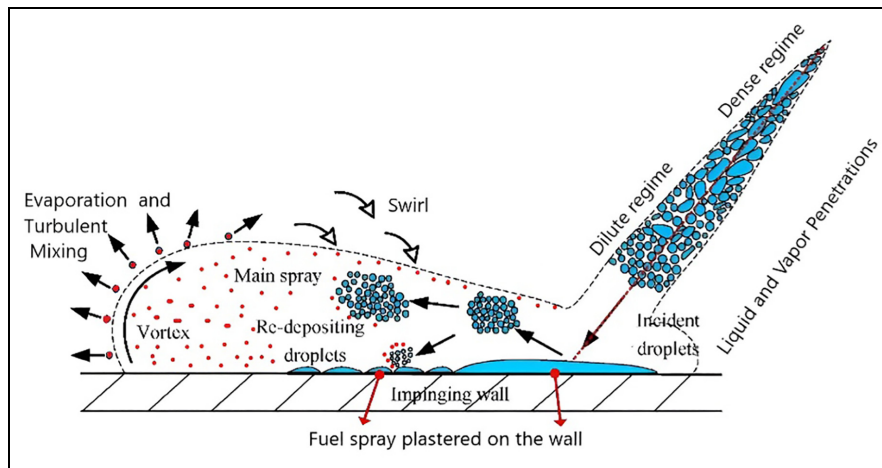Email: ilktemizer@gmail.com

Figure 1. Schematic of fuel droplet on the Wall.[3]

internal combustion engines. Studies on this subject continue at both academic and industrial levels. In studies lasting more than 70 years, no definite finding on turbulence could be determined.[1] For these reasons, it is of great importance to examine the in-cylinder mixture formation, injection dynamics, and the complex structure of the combustion process in the internal combustion engines.[2] Figure 1 shows the wall-fuel distribution interaction.

In order to combustion analysis, it can be done with software bases such as Fortran, C + + , Pascal, where CFD (Computational Fluid Dynamics) codes can be written, as well as commercial software such as STAR-CD, ANSYS, KIVA, FIRE, CFDRC, and VECTIS, which are widely used today.[4,5] As it is known, there are Navier-Stokes equations in the background of all modeling studies. It is mentioned in many studies that the models and equation sets used are reliable and valid.[6–8] Akkus optimized the piston bowl geometry by using CFD. Standard k-ε, Realizable k-ε, and RNG k-ε turbulence models were used to see the effects of the turbulence model on the swirl number. As a result of the analysis of 92 different bowl geometries, power was increased by 5.8% and the bsfc by 5.5%, while NO emissions increased by 15% because of chamber temperatures increase.[9] Sener et al.[10] analyzed five different bowl geometries with a CFD program, and their effects on performance, emission values and combustion characteristics were examined. DE and DF bowl designs were showed better combustion characteristics and lower emission values than other designs. In a similar study, increasing the diameter of the piston bowl positively affects the in-cylinder temperature, pressure, emission, and swirl movement.[11] In addition, the swirl movement of the air has a great effect on combustion and emission.[12] In a study, a lateral swirl combustion system (LSCS) was designed and a conventional ω bowl type was developed. As a result, fuel consumption and soot emission were reduced, while thermal efficiency and combustion performance were increased.[13] Li et al.[14] analyzed the LSCS and DSCS (Double Swirl

Combustion Systems) using the AVL FIRE program. It reported that fuel consumption and soot emissions were reduced with the LSCS geometry. Li et al.[15] seen that the fuel consumption with LSCS was obtained lower by approximately 4–5 g/kWh at each excess air ratio. Also, 1.13%–2.8% improvement in fuel consumption and a 63.4%–70% reduction in soot emissions were achieved while an increase in NOx emission was observed. Thanks to LSCS, the formation of the fuel/air mixture accelerated and the use of air increased because of the swirl.[16,17]

Wei et al.[18] proposed a new swirl formation to improve spray distribution, better mixture quality, and increase airflow movement by using AVL Fire. The best emission values and higher engine performance were achieved at 0.8 swirl rate. A new swirl movement in the combustion chamber of the diesel engine was examined and its effect on emissions was evaluated by using AVL FIRE software. As a result of the necessary optimizations in the bowl geometry, soot and NO_x emissions had been reduced.[16,19] Li et al.[20] modeled two bowl geometries, which the DSCS and MSCS (multi-swirl combustion system) in the AVL FIRE software.[21] Lower thermal load, fuel economy, and emission values were obtained with the DSCS geometry, while the formation of air-fuel mixture, combustion characteristics were improved in the MSCS geometry. Zhou et al.[22] proposed a new separated swirl combustion system (SSCS) to improve the effect of air in the chamber. The SSCS was compared with the DSCS. As a result, higher thermal efficiency and lower brake specific fuel consumption were achieved with the SSCS geometry at different speeds. Park[23] showed that the specific fuel consumption was reduced about 35% with the best bowl geometry by using the KIVA software. Ganji et al.[24] modeled the hemispherical combustion chamber (HCC), shallow depth combustion chamber (SCC), and Toroidal combustion chamber (TCC) geometries by using Converge software. Better air-fuel mixture and homogeneous mixture were provided with TCC bowl depth has 1.26 mm. Mobasheri and Peng[25]

observed that the NO$_x$ emission amount was higher with less depth, and the brake specific fuel consumption was increased for the depth increasing. In another experimental study, the standard combustion chamber geometry of a diesel engine was compared with the HCC, TCC, and TRCC. The TCC geometry compared to the others, it was caused better air-fuel mixture formation and complete combustion as a result of providing higher swirl and squish movement.[26] Also, higher swirl ratio in the piston bowl could be caused to higher cylinder pressure.[27]

In another similar study, Toroidal Re-entrant Combustion Chamber (TRCC), TCC, and HCC and four different spray angles (150°, 155°, 160°, and 165°) were used. The engine performance, mixture formation, fuel consumption, and soot emissions were improved with TRCC type geometry and 160° injection angle.[28] Jyothi and Vijayakumar Reddy[29] created bowl geometries in different designs (Hemispherical, toroidal, and re-entrant toroidal geometries) to create swirl movement in the air. It had been determined that there was a squish flow affecting the turbulence around the compression stroke the TDC with its re-entrant toroidal geometry. Jyothi and Reddy[30] emphasized that swirl, squish, and turbulence gave better results in re-entrant bowl geometry than hemispherical and toroidal geometries. Poulos and Heywood[31] observed that the burning velocity could be increased by changing the bowl geometry. In addition, it was stated that with the increase of turbulence, the burning duration shortened, but the heat losses increased and the thermal efficiency decreased. Nam et al.[32] numerically compared A-type, V-type, and H-type bowl geometries by using the Large Eddy Simulation (LES) technique. As a result, the A-type geometry compared to others provided higher radial velocity and turbulence intensity in the piston bowl. Blank et al. investigated that turbulence by placing two small chambers in addition to the piston bowl. He emphasized that turbulence intensity was more important than the chemical kinetic effect.[33] This designs similar to the A-type bowl geometry was provided that recessed geometries reduce soot emissions and provide fuel economy in diesel engines.[34] As a result, 20% reduction in HC emissions and 24% reduction in CO emissions were achieved, while a slight decrease in engine power was observed. In addition, a significant reduction in the bsfc was detected.

Kalay[35] investigated four different combustion chamber configurations by using Converge CFD software. The piston bowl profile showed that given best results in terms of combustion characteristics had been determined. Boyarski and Reitz conducted a CFD analyses of a diesel engine with a 120° injection angle, they investigated the effects of three different bowl geometry on emissions. Soot was decreased by 89% and NO$_x$ emission was obtained by 86% with the best bowl geometry at 61% EGR opening.[36] Choi et al.[37] designed that the new bowl geometry to have a wide, shallow two-stage bowl that provides adequate spray penetration with the double row nozzle relative to the original bowl geometry. Soot, CO, total HC emissions decreased while NO emissions increased with 60% EGR opening. Gokbel[38] conducted that the MR-1 combustion chamber piston design was made by obtaining the combustion law that provides optimum combustion. 9.6% increase in power, an 8.7% decrease in the bsfc, and a 30% decrease in soot emissions were observed with the piston design in the 3 LD 510 direct injection diesel engine. Moreover, as the pressure was decreased, the stresses, cylinder temperature, and NO$_x$ emissions decreased.[39] The MR combustion mechanism was realized in a double turbulent eddy combustion environment, combines the advantages of both diesel and Otto cycles in a single structure[40,41] Kutlar et al.[42] stated that the geometry of the combustion chamber significantly affects the turbulent burning speeds. Demirci et al.[43] observed that the start of the ignition for MR was later, while the burn duration was shorter than that of the other flat and cylindrical bowl geometries. Moreover, it had been observed that it works more smoothly in leaner mixtures ($\lambda > 1.45$) with MR combustion chamber geometry. According to the test results, as a result of increased the compression ratio and decreased the ignition advance, there was a slight decrease in the mean effective pressure, while the NO emissions were greatly reduced.[44] Unlike the single-rotation combustion chambers of a conventional diesel engine, the MR-process has a double rotation that promotes fuel-air mixture formation, providing ideal evaporation of the fuel spray oriented tangentially to the piston walls. KIVA analysis showed that MR-Process has the potential to achieve better fuel-air mixture, thus increased the engine efficiency while reduced emission levels.[45]

One of the most important parameters determining the mixture formation in the combustion chamber is the geometry of the bowl profile. Bowl geometries that allow in-cylinder airflows have a major impact on fuel-air mixture formation. Unlike the literature in this study, a new combustion chamber as a cyclic analysis was investigated. It was aimed to direct both air movement and fuel spray with the designed bowl geometry. Novel bowl geometries has directional fuel injection feature with wall guided. Thus, the fuel sprays guided to the wall were mixed more evenly and homogeneously to the two adjacent pocket centers. This feature is new and has not been found in the literature. Thanks to this feature, it was ensured that the combustion occurs in the center with the wall guided as a result of the fuel hitting the bowl. This situation improved the mixture formation in the combustion chamber. In addition, a more homogeneous mixture was obtained by providing the distribution of the fuel assembly to more than one region. The directional fuel injection feature in the novel designed chamber geometries was beneficial to turbulence kinetic energy, spray distribution, CO, CO$_2$, and soot emissions.

Material and methods

Numerical study

Testing an engine with the SCC (Standard Combustion Chamber) in different operating conditions is very important in determining the boundary conditions at numerical modeling. Based on the main dimensions and technical specifications of the combustion chamber of the ANTOR 3 LD 510 engine. The analysis of the existing combustion chamber geometry was carried out. In-cylinder heat, flow, mixture formation, and combustion processes were performed in three-dimensional ANSYS FORTE CFD software. Thus, the NCC (New Combustion Chamber) model and the SCC model in the same chamber volume were examined. In this program, time-dependent solutions were carried out in the turbulent flow regime to determine the velocity, pressure, and temperature values. In the design of the bowl geometry, radius (R1 = 11.55, R2 = 5, and R3 = 10.03 mm) were defined for the fuel-air mixture formation and combustion processes. While determining these values, it was taken into consideration that the engine should provide a compression ratio of 17.5. When designing the new combustion chambers, no changes were made to the engine head and injector position, so a piston bowl that did not exist before was designed and positioned taking into account the target of the fuel spray and in-cylinder air movements. The center axes of the piston and the bowl are offset by 2.5 mm due to constructive reasons, and the center axis of the bowl and injector nozzle tip are on the same axis, so different pistons are designed by rotating around the center axis of the bowl. The radius of this pocket formed in the bowl of the piston was matched to the cone center. The designed bowl geometry and SCC were shown in Figure 2. During the compression process in internal combustion engines, the air flow movement in the chamber decreases with the movement of the piston from the BDC to the TDC. This situation also has a significant effect on the mixture formation. NCC type bowl geometry consists of eight (8) pockets as seen in Figure 2. In the three-dimensional CFD analysis, the full model was solved. The simulation conditions were given in Tables 1 and 2. In order to obtain more realistic exhaust emission values, a detailed reduced chemical combustion mechanism had been used, the accuracy of which had been tested in many studies.[7,9,46] RNG k-epsilon turbulence model was used which is more suitable as sub-models in the study. This model offered the opportunity to examine in a macro dimension and provided an advantage over other models in terms of solution time. It is one of the most preferred models for modeling the engines as suggested by some articles.[47,48] Adaptive Collision Mesh model was used for droplet collision. One of the biggest advantages of this model is that it eliminates the dependency on the mesh structure. The KH-RT hybrid model, including the Gas-Jet submodel was used to break up the droplets. The KIVA-based wall collision
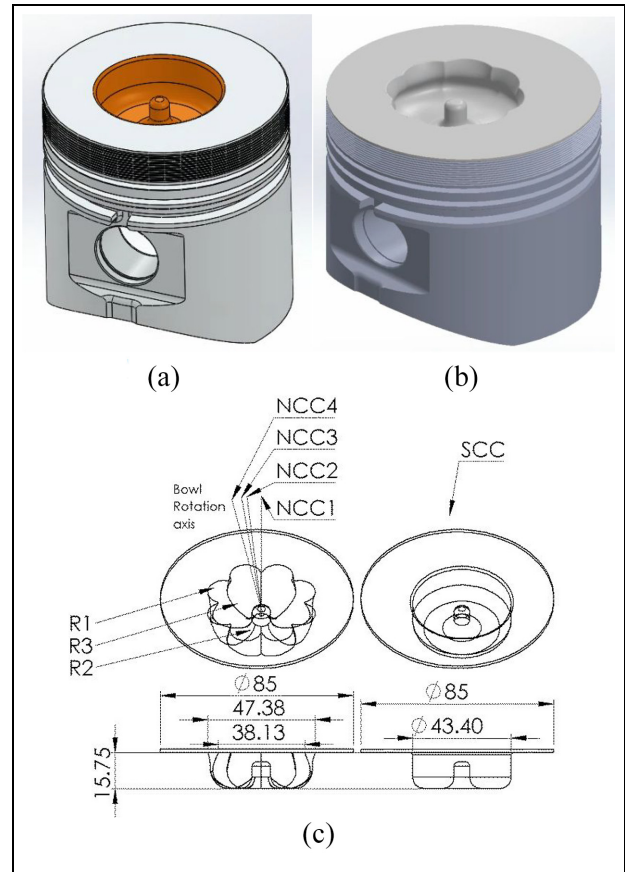

Figure 2. SCC (a), NCC (b), and the technical dimensions of both geometry (c).

Table 1. CFD model parameters.

Bore × Stroke	85 × 90 [mm × mm]
Compression ratio	17.5:1
Nozzles	4 × 0.26 [mm]
Engine IVC	128°CA BCTDC
Engine EVO	134°CA ACTDC
Engine speed	2000 rpm
Fuel injection rate (mass)	5.11 [mg]
Fuel injection timing	15° CA bTDC
(start and stop)	and 9° CA ATDC
Fuel injection temperature	330.15 [K]
Fuel Mean Cone angle	15°
Air inlet temperature at IVC	380 [K]
Air inlet pressure at IVC	1.095 [bar]
Air Swirl ratio at IVC	1.84
Turbulent Kinetic Energy at IVC	95 [m²/sec²]
Turbulance Eddy Dissipation rate at IVC	51 [m²/sec³]
Piston wall temp.	575.15 [K]
Cylinder liner wall temp.	475.15 [K]
Cylinder head wall temp.	550.15 [K]

model developed by Han was used to calculate the fuel droplets colliding with the wall.

The gas-phase working fluids in the combustion engine are modeled as a mixture of individual species, and this composition changes during the engine cycle due to flow convection, molecular diffusion, turbulent

Table 2. Physical and chemical models.

Turbulent flow	Ensemble average flow field in the RANS (Reynolds-Averaged-Navier-Stokes)
Turbulence model	RNG k-epsilon
Wall heat transfer model	Han-Reitz
Wall boundary	Law of the wall
Evaporation model	Discrete Multi component (Ra-Reitz)
Droplet Collision	Adaptive Collision Mesh Model
Droplet Breakup	KH-RT
Soot emission model	Included in detailed mechanism
NO emission model	Included in detailed mechanism
Chemistry	Chemkin based 2 component detailed diesel mechanism (191 species, 1399 reaction)
Fuel	a-methylnaphthalene (a2ch3) %33, n-decane (nc10h22) %67
Air	Ideal gas, atmospheric with %10 residual gas composition

transport, interactions with fuel sprays, and combustion. The conservation equation for the mass of species k is:

$$\frac{\partial \overline{\rho}_k}{\partial t} + \nabla \cdot (\overline{\rho}_k \tilde{\mathbf{u}}) = \nabla \cdot [\overline{\rho} D \nabla \overline{y}_k] + \nabla \cdot \Phi + \dot{\rho}_k^c + \dot{\rho}_k^s (k = 1, \cdots, K) \tag{1}$$

where ρ is the density, subscript k is the species index, K is the total number of species, $\mathbf{u}$ is the flow velocity vector, and $y_k = \rho_k/\rho$ is the mass fraction of species k. Application of Fick's Law of diffusion results in a mixture-averaged molecular diffusion coefficient D. The Φ term accounts for the effects of ensemble-averaging or filtering of the convection term, that is, $\Phi = \overline{\rho}_k \tilde{\mathbf{u}} - \overline{\rho_k \mathbf{u}}$, which has to be modeled. $\dot{\rho}_k^c$ and $\dot{\rho}_k^S$ are source terms due to chemical reactions and spray evaporation, respectively.

In detailed chemical kinetic mechanisms, the reversible (or irreversible) reactions involving K chemical species can be represented in the general form[49,50];

$$\sum_{k=1}^{K} v_{ki}' \chi_k \Leftrightarrow \sum_{k=1}^{K} v_{ki}'' \chi_k (i = 1, \cdots, I) \tag{2}$$
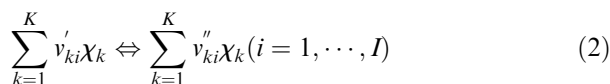
The production rate of the k the species in the i th reaction can be written as,

$$\dot{\omega}_{ki} = \left(v_{ki}'' - v_{ki}' \right) q_i (k = 1, \cdots, K) \tag{3}$$

Where q_i is the rate of progress of reaction i

The summation of $\dot{\omega}_{kr}$ over all the reactions gives the chemical source term $\dot{\rho}_k^c$ in the species continuity equation written as;

$$\dot{\rho}_k^c = W_k \sum_{i=1}^{I} \dot{\omega}_{ki} \tag{4}$$

W_k is the molecular weight

The continuity equation for Turbulent Reactive Flows is as follows (equation (5)).

$$\frac{\partial}{\partial t} + \nabla \cdot (\rho \, \tilde{\mathbf{u}}) = \rho^{\dot{s}} \tag{5}$$

The momentum equation for the fluid (equation (6)) takes into account the effects of convection, pressure force, viscous tension, and turbulent convection, as well as the effect from liquid sprays and mass force.

$$\frac{\partial \overline{\rho}\tilde{\mathbf{u}}}{\partial t} + \nabla \cdot (\overline{\rho}\tilde{\mathbf{u}}\tilde{u}) = -\nabla \overline{p} + \nabla \cdot \overline{\boldsymbol{\sigma}} - \nabla \cdot \boldsymbol{\Gamma} + \overline{\mathbf{F}}^{\mathbf{s}} + \overline{\rho}\mathbf{g} \tag{6}$$

Here, p is the pressure, Fs is the rate of momentum gain per unit volume due to the spray, g is the specific mass force, σ is the Viscous stress tensor given below (7).

$$\overline{\boldsymbol{\sigma}} = \overline{\rho} v \left[\nabla \tilde{\mathbf{u}} + (\nabla \tilde{\mathbf{u}})^{\mathrm{T}} - \frac{2}{3} (\nabla \cdot \tilde{\mathbf{u}}) \mathbf{I} \right] \tag{7}$$

v is laminar kinematic viscosity, I is the descriptor tensor, T is the subindex tensor transpose. Stress; Γ indicates the effects of ensemble averaging or filtering of the nonlinear transport term. In the RANS approximation it is called Reynolds strain, in the LES approximation it is called SGS strain.

According to the first law of thermodynamics, the change of internal energy must be balanced by pressure work and heat transfer. Flow problems with internal combustion engines; Convection of a multicomponent flow must be calculated taking into account the effects of turbulent transport, turbulent attenuation, sprays, chemical reactions, and enthalpy diffusion. Internal energy transport equation (equation (8)):

$$\frac{\partial \overline{\rho}\tilde{I}}{\partial t} + \nabla \cdot (\overline{\rho}\tilde{\mathbf{u}}\tilde{I}) = -\overline{p}\nabla \cdot \tilde{\mathbf{u}} - \nabla \cdot \mathbf{J} - \nabla \cdot \mathbf{H} + \overline{\rho}\overline{\varepsilon} + \dot{Q}^C + \dot{Q}^S \tag{8}$$

I is the specific internal energy, J is the heat flux (equation (9) occurs by heat conduction and enthalpy diffusion),

$$\mathbf{J} = -\lambda \nabla \overline{T} - \overline{\rho} D \sum_{k} \tilde{h}_k \nabla \overline{y}_k \tag{9}$$

λ, T, h_k correspond to the heat transfer coefficient, flow temperature, and specific enthalpy expressions of the species, respectively. ε are turbulent kinetic energy dissipation, and, $\dot{Q}^C$ ve $\dot{Q}^S$ are chemical heat dissipation and spray interaction coefficients, respectively. The H term indicates the effects of ensemble averaging or filtering of the convection term.[49,50]

The fuel assembly was aligned to the nozzles in the designed combustion chamber. A more balanced gas force distribution had been occurred with the combustion in the pockets. No changes were made to the structure and position of the injector. The cone projection was drawn just like in the SCC. One of the main criteria in the new design was the eight pocket radii placed from the top of the piston. While the SCC surface volume is
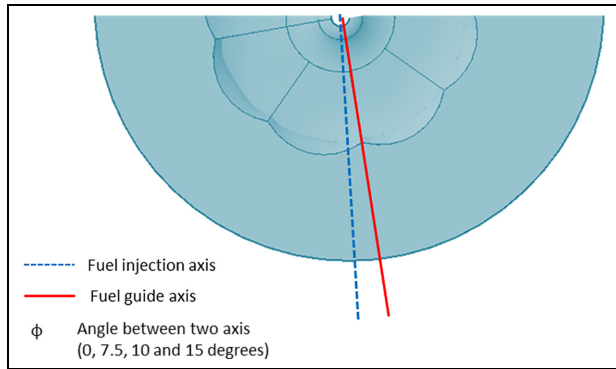
Figure 3. Variation of the spray axis in the combustion chamber.

22.7 mm^3 and the bowl surface area is 3819 mm^2, the NCC the surface volume is 22.7 mm^3 and the bowl surface area is 4020 mm^2 in the Solidworks software. Thanks to NCC, it was aimed that the fuel was plastered on the bowl walls and rapid evaporation of the fuel by utilizing the wall temperature. Another important design criterion was swirl movements. In the numerical analyzes was also seen that the swirl of air in the combustion chamber directed the fuel assembly and affected its structure. The mixture formation was affected by the increasing swirl effect at the end of the intake stroke. Therefore, optimum φ (0°, 7.5°, 10°, and 15°) angles for the Wall Guided Fuel Injection (WGFI) were determined by peripherally the pocket axis at different angles (Figure 3).

Experimental study

In this study, engine performance characteristics and in-cylinder pressure/crank angle (CA) data of ANTOR 3 LD 510 diesel engine by connected to electrical dynamometer were determined. The experimental results obtained contribute both to the determination of the boundary conditions in numerical analysis and the comparison of the results. Thus, the validity and reliability of the results obtained by numerical modeling were tested. Schematic representation of the experimental setup was given in Figure 4. In the experimental results, the combustion analysis of the engine was carried out using the Febris combustion analysis software. Febris combustion analysis software recorded in-cylinder pressures and indicator diagram at different engine speeds (1550, 1700, 1850, 2000, and 2150 rpm) for at least 200 cycles for each test point. The cycle closest to the mean was selected by taking the average of these cycles. Cylinder pressure was measured using OPRANT optical pressure sensor, and the CA was measured by using KUBLER encoder. Table 3 showed the technical specifications of the diesel engine and the uncertainty analysis of experimental measurement devices were given in Table 4.

Result and discussion

Verification of numerical results

In the present study, NCC1, NCC2, NCC3, and NCC4 bowl designs were numerically compared with the SCC chamber geometry. The difference between the NCC1, NCC2, NCC3, and NCC4 designs was the rotation angles of 0°, 7.5°, 10°, and 15° respectively. The three-dimensionally modeled bowl geometries in Ansys FORTE software were examined in terms of in-cylinder pressure and temperature, instantaneous and cumulative heat release rate, exhaust emissions (NO, soot, CO, and CO_2), temperature/spray, and equivalence ratio/spray at different CA's. The numerical analyzes were carried out at 2000 rpm engine speed, at which the maximum brake torque was obtained in the engine. In the study, the engine was operated by using SCC geometry at 2000 rpm and full load. The operating parameters in the experiment were used as the initial conditions in the model, and then the numerical results were verified with
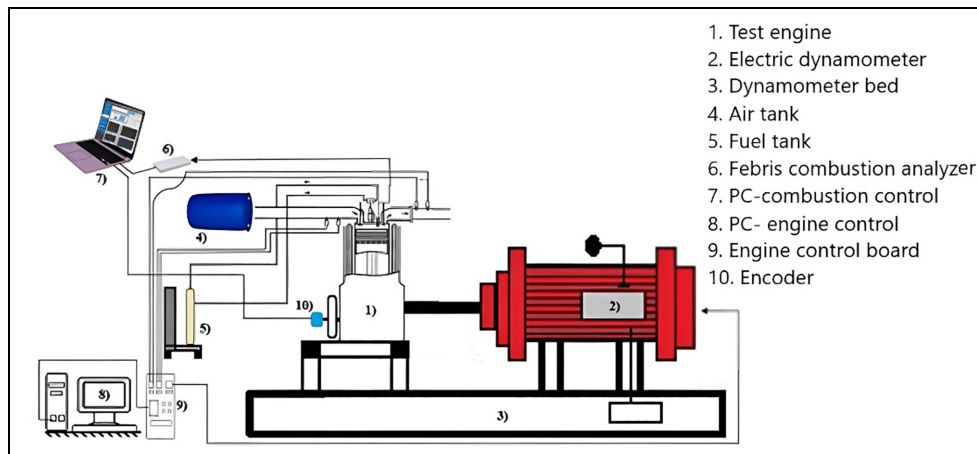

Figure 4. The experimental setup.

Table 3. Technical specifications of experimental engine.

Engine type	4-stroke, direct injection diesel engine
Number of cylinders	1
Cylinder volume	510 cm^3
Bore $\times$ Stroke	85 $\times$ 90 (mm $\times$ mm)
Compression ratio	17.5:1
Maximum power	6.6@3000 (kW)
Maximum torque	32.8@2000 (Nm)
Injection angle	160°
Number of nozzles	4

the experimental results. The characteristic curves of a direct injection diesel engine with SCC are shown in Figure 5. The test engine was operated at full load and at different speeds (1550, 1700, 1850, 2000, and 2150 rpm). Figure 5 shows the torque, bsfc, and exhaust gas temperature variation. In the analyses were chosen 2000 rpm at which the maximum brake torque was obtained. While the maximum engine torque was measured as 32.1 Nm, the bsfc value was measured as 288 g/kWh. The determination of these experimental parameters is an important indicator of the closeness of numerical modeling to reality. The amount of fuel injected per cycle was determined by using the measured torque and the bsfc values, and it used in numerical simulations. In Figure 6, experimental and numerical results were compared in related to in-cylinder pressure and instantaneous heat release rate at 2000 rpm and full load. As could be seen from the results, it had been observed that the obtained results (the parameters obtained for SCC) were close to each other. As a result, the validity and reliability of the modeling were tested for the SCC type. Then, the analysis results of the NCC1, NCC2, NCC3, and NCC4 designs were compared with the SCC geometry results based on the used boundary conditions in the modeling.

Evaluation of in-cylinder parameters with numerical study

Figure 7 shows the variation of in-cylinder pressure and temperature values of different chamber geometry designs according to the CA. Maximum pressure values for SCC, NCC1 ($\varphi = 0$), NCC2 ($\varphi = 7.5$), NCC3 ($\varphi = 10$), and NCC4 ($\varphi = 15$) were calculated as 79.5, 75.2, 78, 78.1, and 78 bar, respectively. In the new design types, it was observed that there was a slight decrease in the combustion pressure. The evaporation degree of the fuel and the mixture formation changed with the NCC type bowl geometries, and it could be said that this was an important factor in the decrease of the maximum pressure. On the other hand, maximum in-cylinder temperatures of SCC, NCC1, NCC2, NCC3, and NCC4 were obtained for the bowl geometries 1766, 1742, 1805, 1817, and 1818 K, respectively (in Figure 7) at 2000 rpm. As can be seen, the highest temperature in the analysis was obtained in the NCC3 bowl geometry. Improvement of mixture formation increases combustion efficiency.[51] The increase in local temperatures in NCC bowl designs compared to SCC is a consequence of this. However, this could not be said for NCC1. The heterogeneous distribution of the fuel drops in the combustion chamber bowls could be said that the caused to deteriorate of combustion and the decrease of local temperatures. On the other hand, the bowl surface area is very important in the piston.[52,53] Increasing the bowl surface area means that the thermal forces on the piston are reduced and the amount of heat transfer from the wall increases. In the numerical study, the total wall heat transfer loss was found to be 134.31, 143.65, 148.58, 148.9, and 148.66 J for the standard, NCC1, NCC2, NCC3, and NCC4, respectively. Moreover, NCC designs showed an increase in heat losses as the fluid velocity in the near-wall region did not change or the swirl ratio decreased. The thermal efficiency was determined as 0.4112, 0.4043, 0.4159, 0.4137, and 0.4187 for the standard, NCC1, NCC2, NCC3, and NCC4, respectively. As can be seen, although the total wall heat transfer loss in the wall has increased in the new combustion chambers, there has been no significant decrease in thermal efficiency.

The instantaneous and cumulative changes in the heat release rates according to the CA were given in Figure 8. The maximum heat release rates (around the TDC) with NCC designs were reduced in both graphs.

Table 4. Uncertainty analysis of measuring devices.

| Pressure sensor	Encoder	Electric dynamometer	Other components
Optrand fiber optic	Cubler	Baturalp Tayland brand brake	Fuel (g) $\pm$0.1%,
Measuring range 0–200 bar	Measuring range 0–12,000 rpm	Maximum torque of 80 Nm	$\Delta P_{air} \pm 0.1\%$
0.025 V/bar sensitivity	Encoder resolution 360 $\times$ 1° CA	% $\pm$ 0.02 Uncertainty	$T_{air} \pm 0.8°C$
120 kHz natural frequency	Converts angle value to digital TTL signal	Torque sensor $\pm$ 10 VDC output	Engine speed (min^{-1}) $\pm$1%
% $\leqslant \pm$ 0.5 accuracy	It can be supplied with 5 V or 120 mA	Powered by 220 V voltage	Time (s) Accuracy $\pm$0.7%
Measurement in temperature range $-40°C$ and 360°C	Measurement in temperature range $-40°C$ and 85°C	Measurement in temperature range $-10°C$ and 60°C	
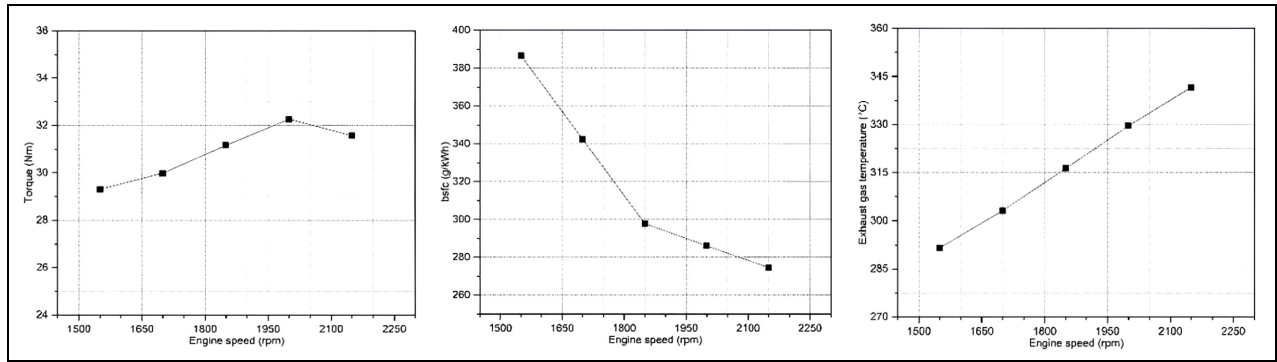
Figure 5. Engine torque, fuel consumption, and exhaust gas temperature variation at the different speeds.
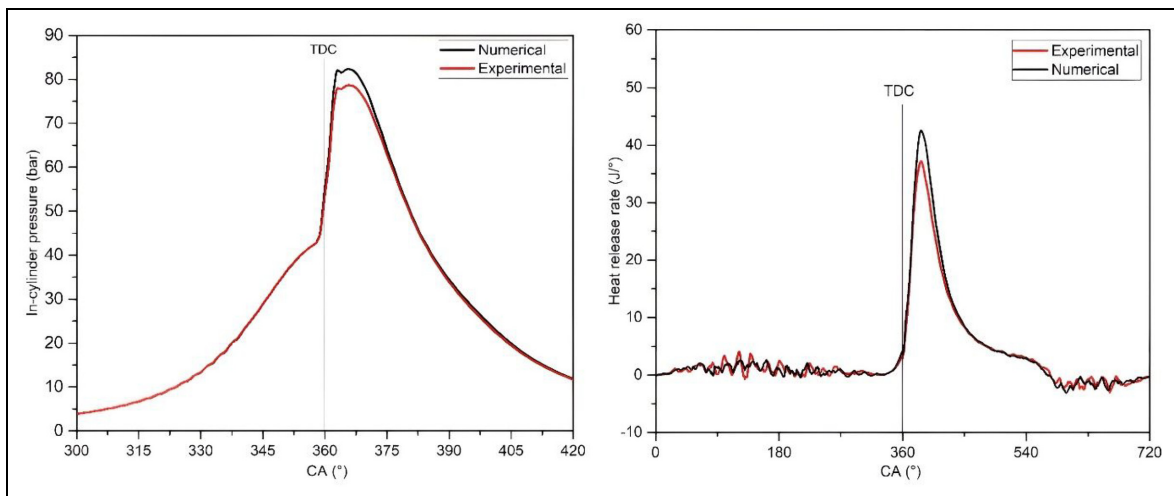

Figure 6. Comparison of p-CA and heat release rate results for experiment and numeric.

This reduction in maximum heat release rates could be considered as a result of local temperatures. In addition, NCC type bowl geometries had a higher surface-volume ratio than SCC, reducing the maximum heat release rates. However, after the TDC (365°–380°), it had been observed that more heat release occurs in all NCC bowl designs compared to the SCC. It could be said that this high heat generated in the controlled combustion phase was effective on incomplete combustion products. This situation is also seen in the cumulative heat release graph.

Figure 9 shows comparison of turbulent kinetic energy (TKE) and swirl ratio over CA for SCC and NCC bowl geometries. When the TKE values were examined, the initial conditions were quite close to each other. Since the only variable was the bowl geometry, it had been observed that higher TKE occurred with the designed new geometries at the BTDC (Before top dead center) and the TDC. As a result of evaporation after the contact of the fuel droplets with the air, TKE decreased at the ATDC (After top dead center). The swirl ratio was lower in NCC chamber geometries (Figure 9). Although the swirl movement was reduced in the NCC combustion chambers, it resulted in better mixture formation and reduced CO emissions. Thus,

the fuel sprays guided to the wall were mixed more evenly and homogeneously to the two adjacent bowl centers. It could be said that this situation was especially effective on CO and soot emissions.[18,46]

The combustion duration was examined for different bowl geometries in Table 5. When 90% of combustion was complete, NCC design geometries had longer combustion duration than SCC type (except for NCC4). It was seen that combustion times are slightly longer in all NCC geometries compared to SCC at 5% and 50% combustion rates, which were accepted as an indicator of the stages where fuel energy was released. Here, for the NCC combustion chamber, it was determined that the fuel burns more slowly and the instantaneous heat release rates decrease around the TDC. It is thought that low swirl rates are effective in the formation of this situation. However, in the later stages of combustion with the piston movement across to BDC (Bottom Dead Center), it was seen that the combustion speed increases, especially in the NCC3 and NCC4 geometries, compared to the SCC. It could be said that the mixture is forced into turbulent combustion tendency by the special geometrical structure of NCC combustion chambers in the expansion stroke. Higher turbulence intensity causes an increase in the surface area of
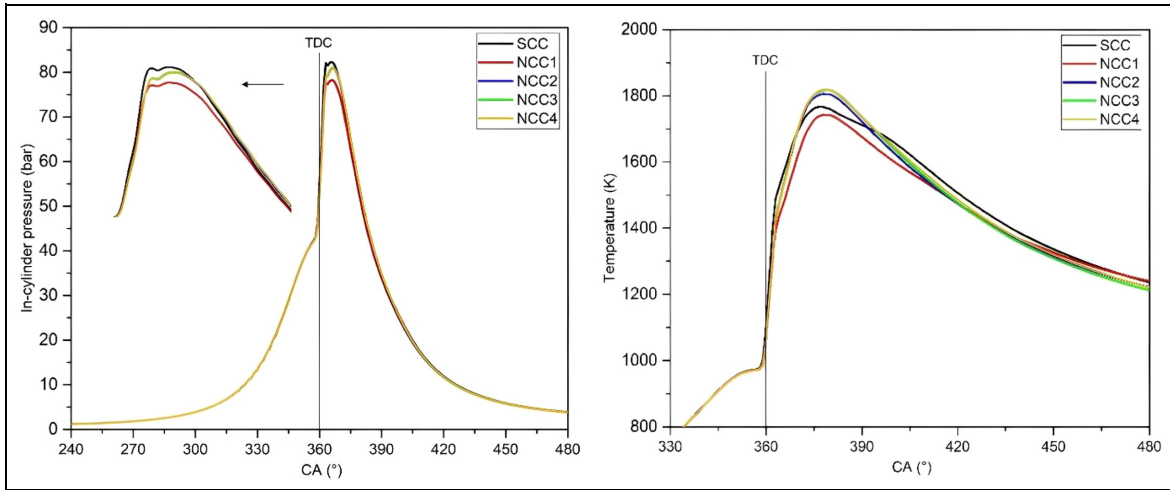
Figure 7. Variation of in-cylinder pressure and temperature according to the CA.
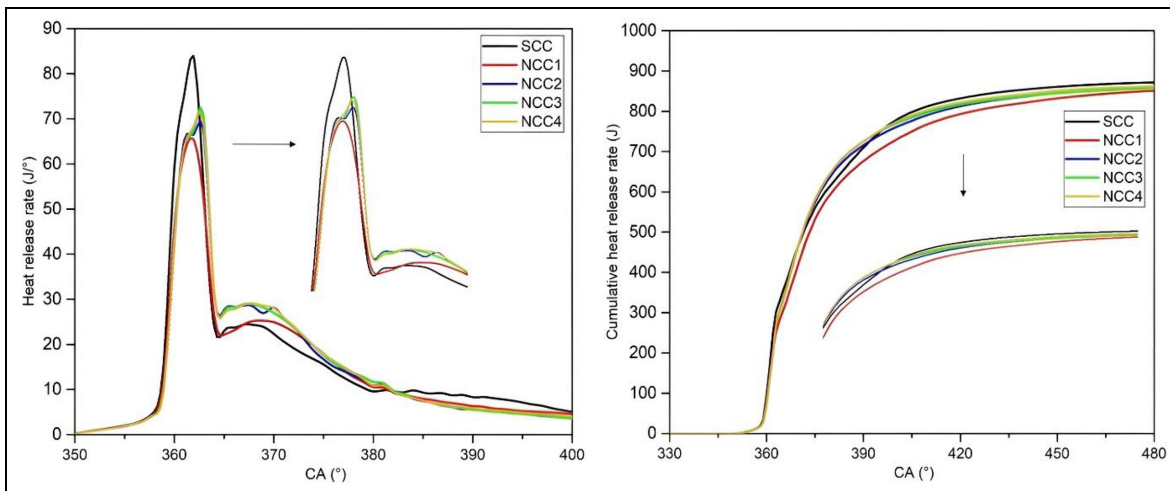

Figure 8. Variation of heat release rate and cumulative heat release rate according to the CA.
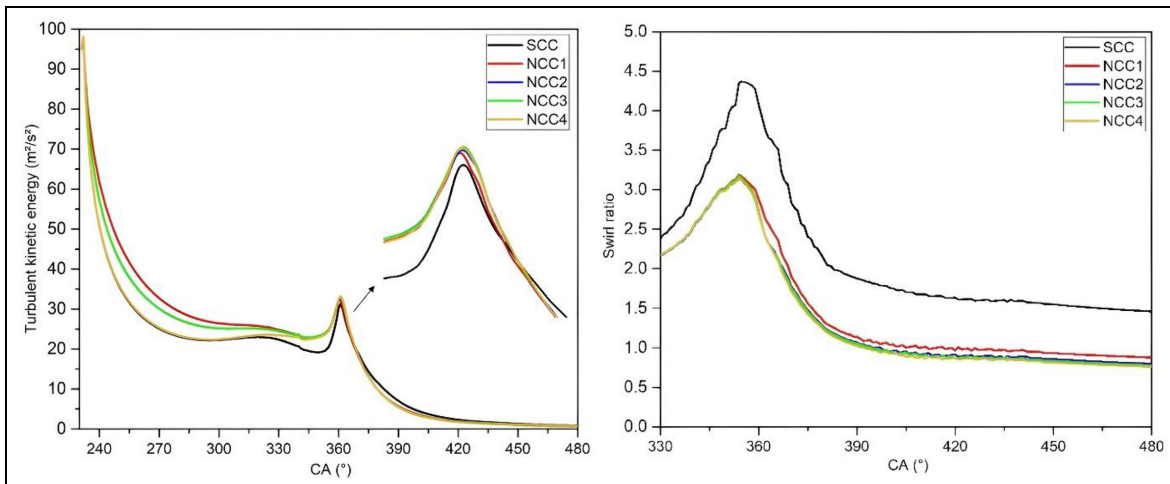

Figure 9. Variation of turbulent kinetic energy and swirl ratio according to the crank angle.

Table 5. Examination of burn duration at different bowl geometries.

Type	Engine speed (rpm)	Load	Combustion duration			
			%5 (ms)	%50 (ms)	%80 (ms)	%90 (ms)
SCC	2000	Full load	0.94	1.708	3.42	4.5
NCC1			0.95	1.842	3.625	5.25
NCC2			0.97	1.725	3.17	4.75
NCC3			1.03	1.79	3.1	4.58
NCC4			0.945	1.74	3.04	4.42
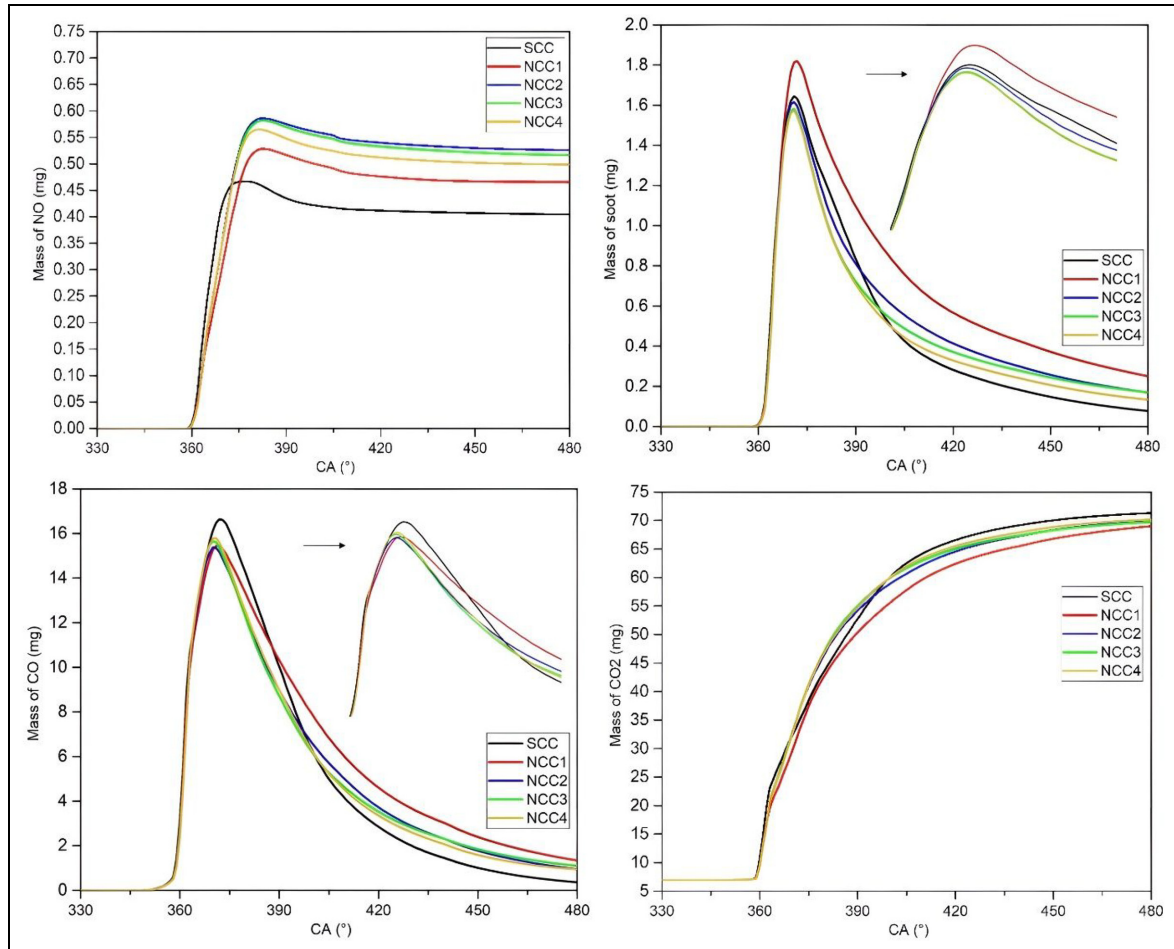
Figure 10. Effect of different designs on exhaust emissions (NO, Soot, CO, and CO_2).

the flame and, as a result, an increase in the combustion rate.[48,54,52] In parallel with the increase in the guided angle of the fuel, it is thought that the distribution of the fuel sprays between the cavities further increases the homogeneity tendency and the wall/fuel interaction. However, this situation is thought to affect the increase in NO emissions.

Exhaust emissions

Figure 10 shows the variation of NO, soot, CO, and CO_2 mass according to the CA for different bowl geometries. NCC design geometries compared to the SCC type, have higher NO emissions. Higher NO was seen in NCC2 and

NCC3. NO emissions are higher in NCC geometries according to the SCC type. It thought that be effectively of the higher turbulence intensity occurring in the fluid velocity and the better mixture formation of fuel with air.[56] As it is known, the formation of carbon atoms, which constitute a large part of soot emissions, is a stage of combustion in diesel engines. Fuel particles sprayed into the combustion chamber under high temperature and pressure decomposes in the form of C-H atoms. While more soot formation was observed for NCC1 ($\varphi = 0$) compared to SCC, lower soot emissions were obtained in the other NCC designs (NCC2, NCC3, and NCC4) with the increase of φ angle and improved mixture formation (Figure 10). The lowest soot formation
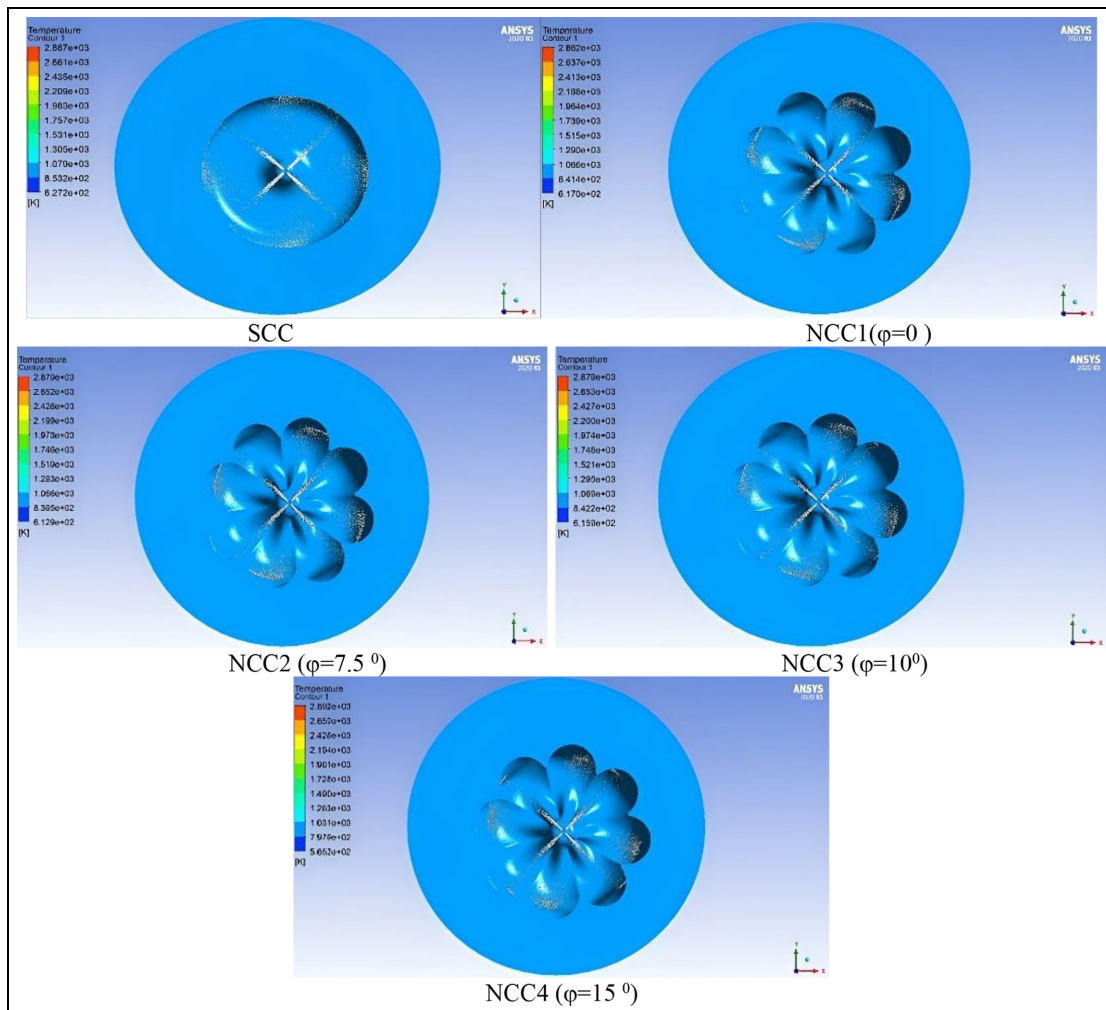
Figure 11. Temperature/spray distribution of different combustion chambers at 360° CA.

was observed in NCC3 and NCC4 bowl geometries. Lower soot emissions had been achieved due to better air-fuel mixture and higher TKE. The soot emissions were reduced with more oxidation in the mixed and late combustion phase. When the CO_2 emissions which was the product of complete combustion were examined, the highest soot was obtained between 360° and 390° CA in NCC3 geometry, while a slight decrease in CO_2 was observed in all NCC geometry types at 390° CA and later. CO emissions occur ATDC and have gradually increased. SCC type according to NCC bowl geometries, maximum CO emissions were obtained ATDC and lower emissions occurred toward the end of the expansion stroke. This could be explained by the in-cylinder temperatures. It could be said that it shows the development parallel to the temperatures. The reason why NCC bowl geometries had lower maximum CO emissions than SCC type was better mixture formation and higher combustion efficiency.

Evaluation of in-cylinder flow parameters

Figures 11 and 12 show the temperature/spray distributions of different combustion chambers at CA's of 360°

and 370°, respectively. When the results were examined, it was seen that the maximum temperatures were close to each other for all combustion chambers. However, the distribution of the fuel assembly and the enhanced combustion phenomenon caused the local temperatures to change. With the change of the φ angle, it completely affected the distribution of the fuel assembly in the combustion chamber. Analyzing especially the temperature/spray distributions in Figure 12, a counterclockwise flow of fuel particles has occurred for all bowl geometries. There was attributed to the swirl effect that occurs in the chamber. Fuel droplets appearing in all figures represent liquid form. Therefore, combustion chamber temperatures should be commented by examining their equivalence ratio. When Figure 12 is examined, it is seen that the local temperature distributions are equal in some combustion chambers and different in others. In the NCC1 geometry was observed that different temperatures occur in all adjacent pocket regions. This result was accepted as an indicator of heterogeneous distribution. However, it was seen in NCC2, NCC3, and NCC4 bowl geometries that homogeneous distribution was achieved with increasing φ angle and a temperature distribution spreads throughout the combustion chamber.
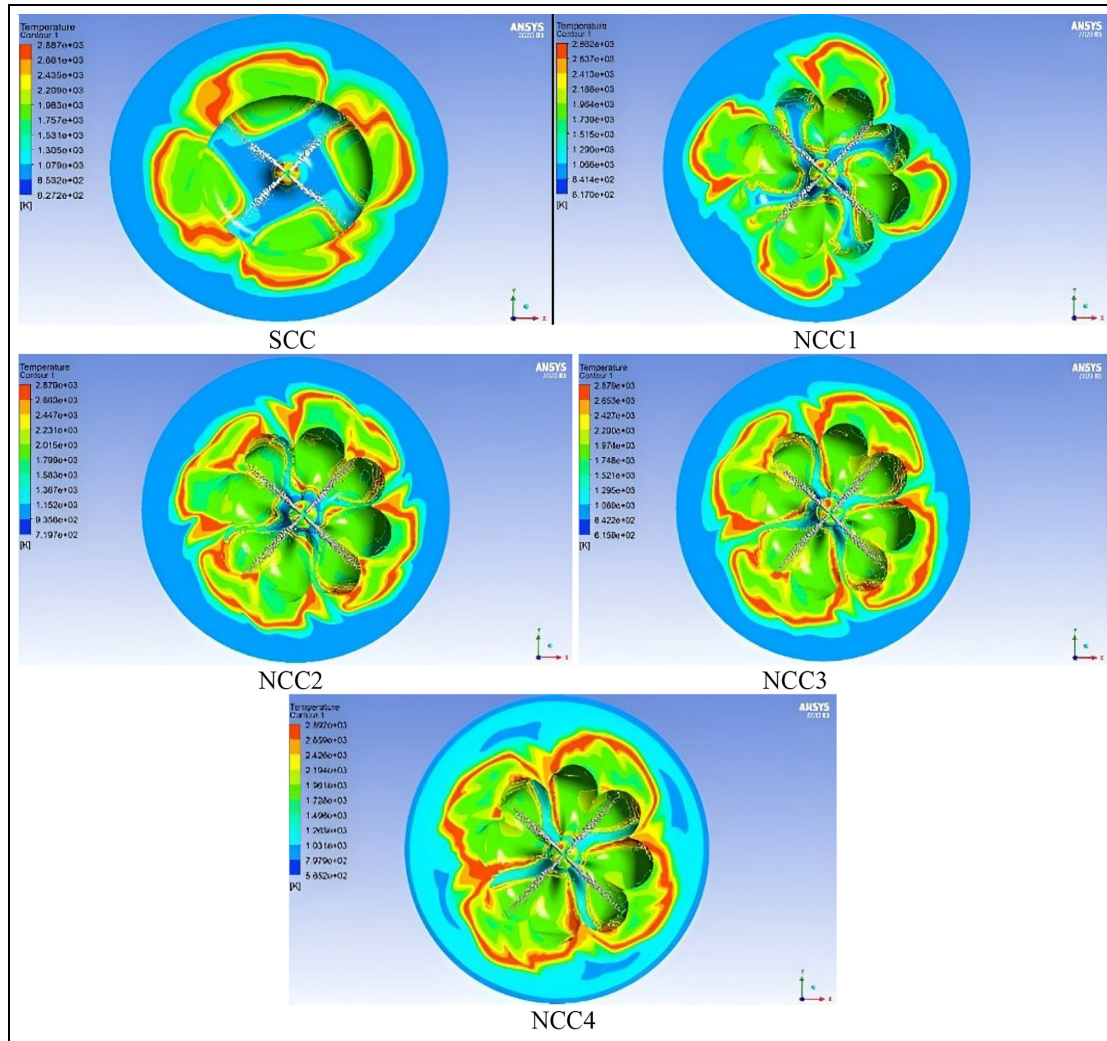
Figure 12. Temperature/spray distribution of different combustion chambers at 370° CA.

The increase in mass transferred to the combustion chamber increases the mixture formation over time.[47] Equivalence distributions spreading over a wider area were obtained for NCC2, NCC3, and NCC4 geometries. This fuel distribution had been considered as one of the important parameters in the formation of CO and soot emissions. Figures 13 and 14 show the equivalence ratios/spray distributions of different combustion chambers at CA's of 360° and 370°, respectively. It was seen that there is a fuel (in the swirl direction) condensation to the left of the region where the fuel assembly hits. In the SCC type, a total of four different fuel densities could be seen to occur on the left side of the areas where the fuel assembly hits at the 370° crank position. In the NCC1 bowl geometry, there was a heterogeneous distribution in all adjacent pockets. In the combustion chambers (such as NCC2 and NCC4) where the fuel distribution was guided into the pockets and separated homogeneously, a fuel distribution that spreads almost throughout the combustion chamber could be mentioned.

Conclusion

In the present study, NCC1, NCC2, NCC3, and NCC4 bowl designs were numerically compared with the SCC geometry. The difference between the NCC1, NCC2, NCC3, and NCC4 designs was the rotation angles of 0°, 7.5°, 10°, and 15° respectively. As a result, the validity and reliability of the modeling were tested. Obtained results are listed below as items.

- The pressure reduction in the new design chamber geometries caused the engine to run more quietly and smoothly, resulting in a decrease in the thermal and mechanical loads on the engine parts.
- The heat release rates decreased with NCC designs because of local temperatures and higher surface-volume ratio. However, more heat release occurred in the NCC bowl designs (except NCC1) compared to the SCC at between 365° and 380° CA. In this CA range, for SCC, NCC1, NCC2, NCC3, and NCC4 geometries were obtained 617, 596, 640, 649, and 649 J, respectively.
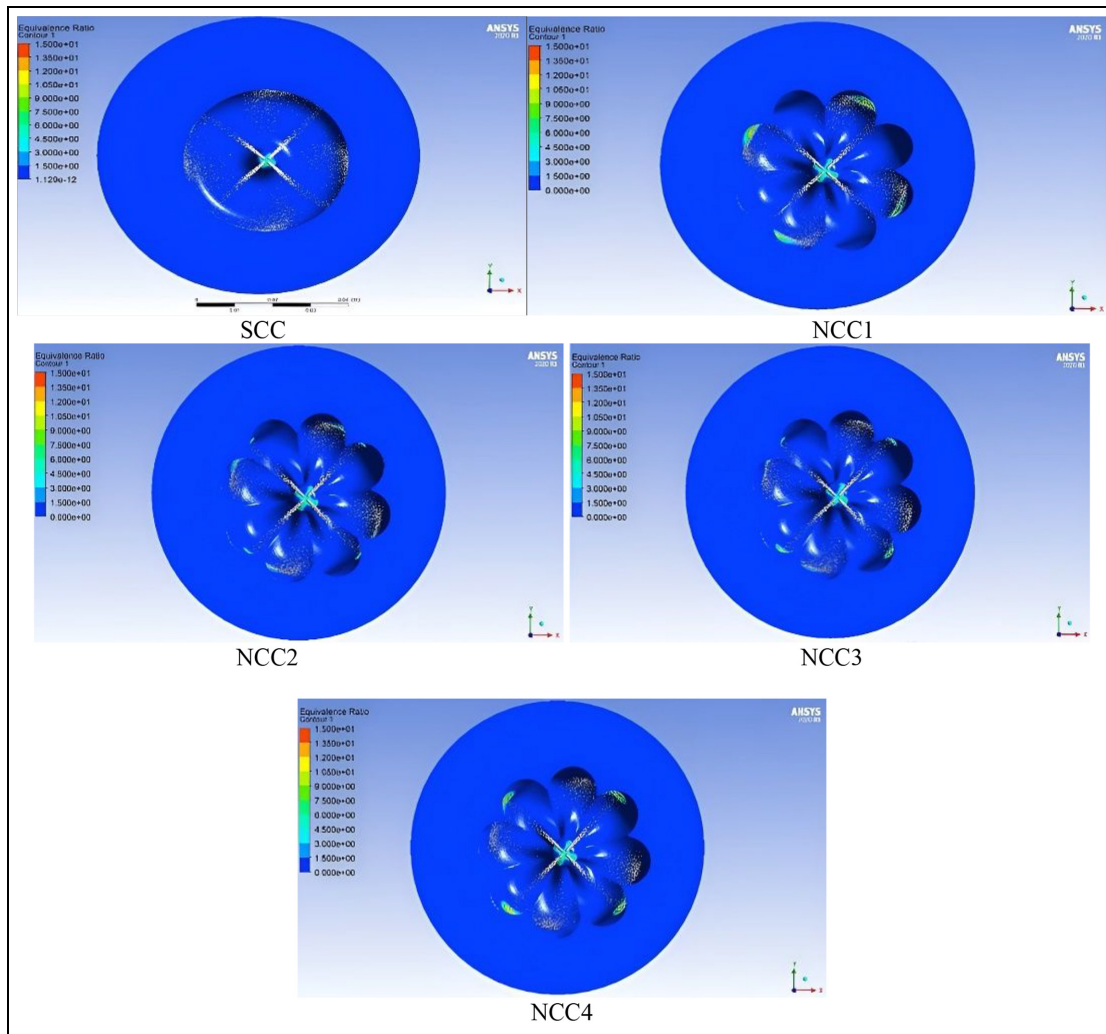
Figure 13. Equivalence ratio/spray distribution of different combustion chambers at 360° CA.

- While lower soot, CO and CO_2 were obtained with NCC bowl geometries (except NCC1) than the SCC type, NO emissions increased. It is thought that the radius geometry determined in the fuel guide wall and combustion chambers increases the distribution of fuel sprays in the chamber and their interaction with the air (for NCC3-NCC4), thus improving the mixture formation as a result of fuel spray movement. The fuel assembly was examined with temperature/ spray and equivalence/spray distribution at different CA's. In the NCC2, NCC3, and NCC4 temperature distributions, the local temperatures increased and a more homogeneous mixture was obtained.

- As a result, NCC bowl geometries outperformed the standard bowl geometry in terms of turbulent kinetic energy, spray distribution, CO, CO_2, and soot emissions. The best engine parameters were obtained with NCC3 bowl geometry.
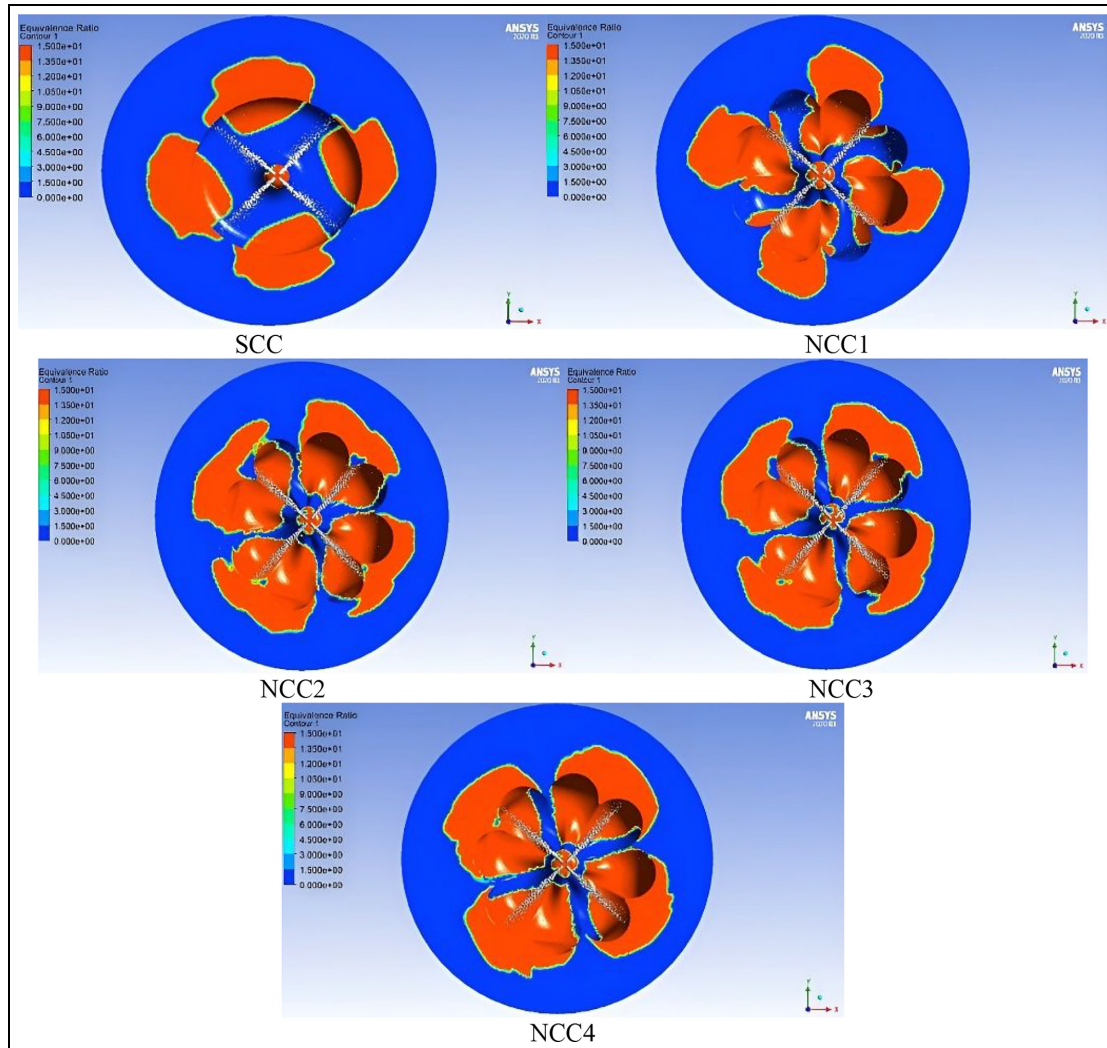
Figure 14. Equivalence/spray distribution of different combustion chambers at 370° CA.

ORCID iDs

İlker Temizer https://orcid.org/0000-0003-1170-3898
Ömer Cihan https://orcid.org/0000-0001-8103-3063

References

1. Atak S. *Effects of different combustion chamber geometries on turbulent flame speed.* Master's thesis, Institute of Science and Technology, Istanbul Technical University, Istanbul, Turkey, 2018.
2. Johnson TV. Review of diesel emissions and control. *Int J Engine Res* 2009; 10(5): 275–285.
3. Lua H, Nishida K, Uchitomi S, Ogata Y, Zhang W and Fujikawa T. Effect of temperature on fuel adhesion under spray-wall impingement condition. *Fuel* 2018; 234: 56–65.
4. Sridhar G, Paul PJ and Mukunda HS. Simulation of fluid flow in a high compression ratio reciprocating internal combustion engine. *Proc IMechE, Part A: J Power and Energy* 2004; 218(6): 403–416.
5. Basha SA and Gopal KR. In-cylinder fluid flow, turbulence and spray models-a review. *Renew Sustain Energy Rev* 2009; 13(6–7): 1620–1627.
6. Colin O and Benkenida A. The 3-zones Extended Coherent Flame Model (ECFM3Z) for computing premixed/diffusion combustion. *Oil Gas Sci Technol* 2004; 59(6): 593–609.
7. Askarova A, Bolegenova S, Maximov V, et al. Investigation of the different Reynolds numbers influence on the atomization and combustion processes of liquid fuel. *Bulg Chem Commun* 2018; 50: 68–77.
8. Temizerİ, CihanÖ and Eskici B. Numerical and experimental investigation of the effect of biodiesel/diesel fuel on combustion characteristics in CI engine. *Fuel* 2020; 270: 117523.

9. Akkuş C. *Optimization of piston bowl geometry in terms of fuelconsumption and emissions using computational fluiddynamics in a diesel engine*. Master's thesis, Institute of Science and Technology, TOBB University of Economics and Technology, Ankara, Turkey, 2020.

10. Şener R, Özdemir MR and Yangaz MU. Influence of piston bowl geometry on combustion and emission characteristics. *Proc IMechE, Part A: J Power and Energy* 2019; 233(5): 576–587.

11. Abdul Gafoor CP and Gupta R. Numerical investigation of piston bowl geometry and swirl ratio on emission from diesel engines. *Energy Convers Manag* 2015; 101: 541–551.

12. Benajes J, Molina S, García JM and Riesco JM. The effect of swirl on combustion and exhaust emissions in heavy-duty diesel engines. *Proc IMechEng, Part D: J Automobile Engineering* 2004; 218(10): 1141–1148.

13. Chen Y, Li X, Li X, Zhao W and Liu F. The wall-flow-guided and interferential interactions of the lateral swirl combustion system for improving the fuel/air mixing and combustion performance in DI diesel engines. *Energy* 2019; 166: 690–700.

14. Li X, Chen Y, Su L and Liu F. Effects of lateral swirl combustion chamber geometries on the combustion and emission characteristics of DI diesel engines and a matching method for the combustion chamber geometry. *Fuel* 2018; 224: 644–660.

15. Li XR, Zhou H, Su L, Chen Y, Qiao Z and Liu FS. Combustion and emission characteristics of a lateral swirl combustion system for DI diesel engines under low excess air ratio conditions. *Fuel* 2016; 184: 672–680.

16. Su L, Li X, Zhang Z and Liu F. Numerical analysis on the combustion and emission characteristics of forced swirl combustion system for di diesel engines. *Energy Convers Manag* 2014; 86: 20–27.

17. Maurya RK and Agarwal AK. Experimental investigation on the effect of intake air temperature and air-fuel ratio on cycle-to-cycle variations of HCCI combustion and performance parameters. *Appl Energy* 2011; 88(4): 1153–1163.

18. Wei S, Wang F, Leng X, Liu X and Ji K. Numerical analysis on the effect of swirl ratios on swirl chamber combustion system of di diesel engines. *Energy Convers Manag* 2013; 75: 184–190.

19. Prasad BV, Sharma CS, Anand TNC and Ravikrishna RV. High swirl-inducing piston bowls in small diesel engines for emission reduction. *Appl Energy* 2011; 88(7): 2355–2367.

20. Li X, Sun Z, Du W and Wei R. Research and development of Double Swirl combustion system for a di diesel engine. *Combust Sci Technol* 2010; 182(8): 1029–1049.

21. Li X, Qiao Z, Su L, Li X and Liu F. The combustion and emission characteristics of a multi-swirl combustion system in a DI diesel engine. *Appl Therm Eng* 2017; 115: 1203–1212.

22. Zhou H, Li X, Zhao W and Liu F. Effects of separated swirl combustion chamber geometries on the combustion and emission characteristics of DI diesel engines. *Fuel* 2019; 253: 488–500.

23. Park SW. Optimization of combustion chamber geometry for stoichiometric diesel combustion using a micro genetic algorithm. *Fuel Process Technol* 2010; 91(11): 1742–1752.

24. Ganji PR, Singh RN, Raju VRK and Srinivasa Rao S. Design of piston bowl geometry for better combustion in direct-injection compression ignition engine. *Sadhana* 2018; 43(6): 92.

25. Mobasheri R and Peng Z. CFD investigation of the effects of re-entrant combustion chamber geometry in a HSDI diesel engine. *Int J Mech Aerospace Ind Mechatron Manuf Eng* 2013; 7(4): 770–780.

26. Karthickeyan V. Effect of combustion chamber bowl geometry modification on engine performance, combustion and emission characteristics of biodiesel fuelled diesel engine with its energy and exergy analysis. *Energy* 2019; 176: 830–852.

27. Sushma H and Jagadeesha KB. CFD modeling of the in-cylinder flow in direct-injection diesel engines. *Int J Sci Res Publ* 2013; 3(12): 1–7.

28. Khan S, Panua R and Bose PK. Combined effects of piston bowl geometry and spray pattern on mixing, combustion and emissions of a diesel engine: a numerical approach. *Fuel* 2018; 225: 203–217.

29. Jyothi US and Vijayakumar Reddy K. Experimental study on performance, combustion and emissions of diesel engine with re-entrant combustion chamber of aluminum alloy. *Mater Today Proc* 2017; 4(2): 1332–1339.

30. Jyothi US and Reddy KVK. Effect of combustion chamber geometry on performance and combustion characteristics of hydrogen enriched diesel engine. *Int J Appl Eng Res* 2018; 13(10): 7998–8004.

31. Poulos SG and Heywood JB. International congress exposition detroit, Michigan. *Soc Automot Eng* 1983; 89/776: 830334.

32. Nam SM, Lee KB and Rhi SH. Effect of piston bowl shape on the in-cylinder flow characteristics of IC engines. *J Mech Sci Technol* 2014; 28(6): 2377–2384.

33. Blank DA, Pouring AA and Lu J. Qualitative flow field studies of combustion in I.C. Engines using a simplified sonex bowl-in-piston geometry. SAE paper 2001-01–00, 2001.

34. Saito T, Daisho Y, Uchida N and Ikeya N. Effects of combustion chamber geometry on diesel combustion. SAE paper 861186, 1986.

35. Kalay I. *Investigation of piston bowl in diesel engines*. Master's thesis, Institute of Science and Technology, Istanbul Technical University, Istanbul, Turkey, 2016.

36. Boyarski NJ and Reitz RD. Premixed Compression Ignition (PCI) combustion with modeling-generated piston bowl geometry in a diesel engine. SAE paper 2006-01-0198, 2006.

37. Choi S, Shin SH, Lee J, Min K and Choi H. The effects of the combustion chamber geometry and a double-row nozzle on the diesel engine emissions. *Proc IMechE, Part D: J Automobile Engineering* 2015; 229(5): 590–598.

38. Gokbel R. *Modernization of the Antor 3LD 510 diesel engine applying of the new (MR-1) single swirl type combustion chamber and intake port geometry*. Master's thesis, Institute of Science and Technology, Istanbul Technical University, Istanbul, Turkey, 2008.

39. Kavruk KO. *Investigation of using the MR-1 combustion chamber and the effects to the in-cylinder parameters and performance on the Antor 3LD 510 diesel engine*. Master's thesis, Institute of Science and Technology, Istanbul Technical University, Istanbul, Turkey, 2008.

40. Mehdiyev R, Ogun K, Ozcan E, et al. The twin swirl "mR-Process" combustion mechanism and conversion of

diesel engines to operate with gaseous fuels. SAE paper 2011-24-00, 2011.

41. Mehdiyev R, Alkan AD, Ünar M and Karataş Ö. An alternative superior combustion mechanism that can convert domestic production marine diesel engines to 100% natural gas fuels. *GMO J Ship Mar Technol* 2017; 207: 49–65.

42. Kutlar OA, Doğan HE, Demirci A and Arslan H. An investigation of the impact of combustion chamber geometry on turbulent burning speeds in a thermodynamic model. *J Energy Resour Technol* 2023; 145(6): 1–10.

43. Demirci A, Doğan HE, Kutlar OA, Cihan Ö and Arslan H. Investigation of burn parameters and cyclic variations of a spark ignition engine with different combustion chambers. *J Energy Resour Technol* 2023; 145(5): 1–10.

44. Demirci A, Doğan HE, Cihan Ö, Kutlar OA, Mehdiyev R and Arslan H. The effects of different compression ratios and spark advances on the performance and emissions of a spark ignition engine with a new combustion chamber. *Sakarya Univ J Sci* 2017; 21(5): 932–942.

45. Calik AT, Taskiran OO and Mehdiyev R. Numerical investigation of twin swirl application in diesel engine combustion. *Fuel* 2018; 224: 101–110.

46. Liu D, Li X, Shang H, Xie L, Chen Y and Chang J. Combustion performance and fuel injection timing adaptability of a lateral swirl combustion system for direct injection diesel engines. *Fuel* 2021; 286: 120663.

47. Jaichandar S and Annamalai K. Influences of re-entrant combustion chamber geometry on the performance of Pongamia biodiesel in a DI diesel engine. *Energy* 2012; 44: 633–640.

48. Temizer I, Cihan O and Öncüoğlu Ö. Numerical investigation of different combustion chamber on flow, combustion characteristics and exhaust emissions. *Eur Mech Sci* 2023; 7(1): 7–15.

49. Trivedi S and Cant RS. Turbulence intensity and length scale effects on premixed turbulent flame propagation. *Flow Turbul Combust* 2022; 109: 101–123.

50. Murakami A, Sakimoto M, Arai M and Hiroyasu H. Measurement of turbulent flow in the combustion chamber of a D.I. Diesel engine. SAE paper 900061, 1990.

51. Payri F, Benajes B, Margot X and Gil A. CFD modeling of the in cylinder flow in direct-injection Diesel engines. *Comput Fluids* 2004; 33: 995–1021.

52. Yaldız E. *Investigation of the nitrogen oxides formation experimentally and theoretically in a diesel engines.* Master's thesis, Istanbul Technical University, Turkey, 2012.

53. Amsden AA, O'Rourke PJ and Butler TD. KIVA-II: a computer program for chemically reactiveflows with sprays. *Los Alamos National Laboratory Report LA-11560-MS, Los Alamos NationalLaboratory*, 1989.

54. Ansys Forte theory manual basic governing equations. Ansys; R2, https://www.scribd.com/document/536366549/ANSYS-Forte-Theory-Manual-18-2 (2020, accessed 1 December 2021).

55. Periyasamy S and Alwarsamy T. Analysis of Block vibrations induced by combustion chamber pressure in a diesel engine. *J Vibroeng* 2012; 14(1): 250–259.

56. Periyasamy S and Alwarsamy T. Combined effects of inertia and pressure on engine vibration. *J Vib Control* 2012; 19(16): 2469–2480.

Appendix

Notation

SCC	Standard Combustion Chamber
NCC	New Combustion Chamber
NCC1	New Combustion Chamber 1
NCC2	New Combustion Chamber 2
NCC3	New Combustion Chamber 3
NCC4	New Combustion Chamber 4
CA	Crank Angle
SoC	Start of Combustion
(EoC)	End of Combustion
ID	Ignition Delay
RNG	Renormalisation Group
KH-RT	Kelvin-Helmholtz Rayleigh-Taylor
ECFM	Extended coherent flame model
ATDC	After Top Dead Center
BDC	Bottom Dead Center
CTDC	Combustion Top Dead Center